NANO LETTERS

Letter

pubs.acs.org/NanoLett

Origin of Size Dependency in Coherent-Twin-Propagation-Mediated Tensile Deformation of Noble Metal Nanowires

Jong-Hyun Seo,[†,‡,▽] Harold S. Park,[§,▽] Youngdong Yoo,[∥] Tae-Yeon Seong,[‡] Ju Li,[⊥,¶] Jae-Pyoung Ahn,*[,†] Bongsoo Kim,*[,∥] and In-Suk Choi*[,#]

[†]Advanced Analysis Center, KIST, Seoul 136-791, Korea

[‡]Department of Materials Science and Engineering, Korea University, Seoul 136-701, Korea

[§]Department of Mechanical Engineering, Boston University, Boston, Massachusetts 02215, United States

[∥]Department of Chemistry, KAIST, Daejeon 305-701, Korea

[⊥]Department of Nuclear Science and Engineering and [¶]Department of Materials Science and Engineering, Massachusetts Institute of Technology, Cambridge, Massachusetts 02139, United States

[#]High Temperature Energy Materials Research Center, KIST, Seoul 136-791, Korea

Supporting Information

ABSTRACT: Researchers have recently discovered ultrastrong and ductile behavior of Au nanowires (NWs) through long-ranged coherent-twin-propagation. An elusive but fundamentally important question arises whether the size and surface effects impact the twin propagation behavior with a decreasing diameter. In this work, we demonstrate size-dependent strength behavior of ultrastrong and ductile metallic NWs. For Au, Pd, and AuPd NWs, high ductility of about 50% is observed through coherent twin propagation, which occurs by a concurrent reorientation of the bounding surfaces from {111} to {100}. Importantly, the ductility is not reduced with an increase in strength, while the twin propagation stress dramatically increases with decreasing NW diameter from 250 to 40 nm. Furthermore, we find that the power-law exponent describing the twin propagation stress is fundamentally different from the exponent describing the size-dependence of the yield strength. Specifically, the inverse diameter-dependence of the twin propagation stress is directly attributed to surface reorientation, which can be captured by a surface energy differential model. Our work further highlights the fundamental role that surface reorientations play in enhancing the size-dependent mechanical behavior and properties of metal NWs that imply the feasibility of high efficiency mechanical energy storage devices suggested before.

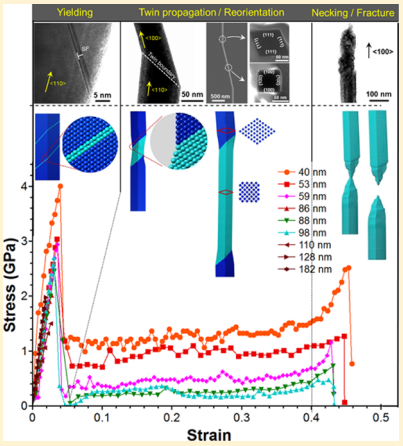

KEYWORDS: *Nanowires, ultrastrong and ductile, twin propagation, size effect, surface energy*

The question of how the mechanical properties of metallic materials change as their characteristic sizes are reduced to nanometer dimensions has recently attracted significant scientific interest.[1−3] In an attempt to answer this fundamental question, the mechanical behavior of single crystalline metal nanowires (NWs) under tensile loading has been extensively studied primarily using classical molecular dynamics,[1,4] and many resulting predictions of unique mechanical behavior emerges specifically as a result of the nanometer dimensionality.

Experimental investigation into this question has also been explored through recent advances in the synthesis of dislocation-free, single-crystalline metal NWs.[5−7] However, due to a range of experimental difficulties related to manipulating and applying loads to nanosized objects, there have been comparably few experimental reports on the tensile stress-induced plastic deformation of metal NWs.[5,8−13] While most of previous experimental studies found that metal NWs exhibit very high strength,[5,9,11−14] they also observed that the subsequent failure of the NWs was almost always brittle, typically with fracture strains less than 5%,[5,14] and some reporting fracture strains in the 10−15% range.[11−13] In contrast, a recent study from our group reported unique and highly desirable combination of ultrastrong and ductile behavior of Au NWs with fracture strains near 50% through twin propagation,[9] as was predicted by classical molecular dynamics for other face-centered cubit (fcc) metals.[15−19]

Some fundamental questions are still to be resolved. Can we observe size-dependent mechanical properties in these ultrastrong and ductile metallic NWs? Is there any difference in the size-dependent behavior between yielding and twin propagation? Can we conclusively establish a direct connection between concurrent geometric and surface reorientations

Received: June 21, 2013
Revised: September 8, 2013
Published: September 27, 2013

   dx.doi.org/10.1021/nl402282n | *Nano Lett.* 2013, 13, 5112−5116

during plastic deformation and the size-dependent mechanical properties under tensile loading for NWs?

In this work, we present answers to these key questions through in situ tensile testing of single crystalline Au, Pd, and AuPd NWs with diameters of 40−250 nm. Interestingly, we find that the size-dependent behavior of twin propagation is different from that of yielding. Furthermore, we theoretically associate the stress required for twin propagation (twin propagation stress) with the surface energy change resulting from the tensile stress-induced reorientation of the NW from {111} to {100}, thereby explaining the experimentally observed inverse proportionality of the twin propagation stress to the NW diameter. We also find that the energetic cost of the surface reorientation becomes important at a critical NW diameter of ∼100 nm at which point the twin propagation stress increases substantially. Our results unambiguously demonstrate the fundamental role that surface reorientations play in enhancing the size-dependent mechanical behavior and properties of metal NWs and imply the feasibility of high-efficiency mechanical energy storage devices and shape memory application of NWs suggested by a number of theoretical studies.[15−19]

Defect-free single crystalline Au, Pd, and AuPd NWs with diameters ranging from 40 to 250 nm and lengths of 5 to 20 μm were synthesized using the vapor transport method.[6,7] The detailed structural information of the as-grown NWs was given in our previous works,[6,7] where high-resolution TEM (HRTEM) images and selected area electron diffraction (SAED) patterns showed the single crystalline and twin-free nature of the vertically grown NWs. The NWs all have a ⟨110⟩ axial growth direction and a rhombic cross-section bounded by four equivalent close-packed {111} transverse surfaces. The in situ tensile tests were carried out in a dual beam electron microscope (FEI). To apply tensile loading, one end of the NW was fixed to a nanomanipulator (MM3A, Kleindeck) tungsten tip and the other end to a silicon cantilever as part of a force measurement system (FMS, Kleindeck) by FIB Pt deposition. The NW was subsequently pulled in tension at a displacement rate of 1.9×10^{-7} m/sec (see also Supporting Information Movie S1 and S2).

Ultrastrong and ductile tensile deformation process was clearly observed for Pd and AuPd NWs as well as for Au NWs, consistent with predictions by molecular dynamics (MD) simulations for other fcc metal NWs.[16−18] A representative deformation behavior of the Pd NW is illustrated via the TEM and SEM images and the three-stage stress−strain curve in Figure 1 (see also Supporting Information Movie S1). In the yielding stage (stage 1), the initially rhombic cross section of the ⟨110⟩ NW with {111} transverse surfaces (⟨110⟩/{111}NW) deforms elastically until the stress drops because of the nucleation of a twin (the yield stress). The plateau stress−strain region that defines the twin propagation stage (stage 2) appears due to the stress-induced propagation of the twin boundary along the NW length of more than 1 μm. SAED patterns of the original and twinned regions (Supporting Information Figure S1b−d) show that the twin formation reorients the lattice of the NW from ⟨110⟩ to ⟨100⟩. The twin propagation results in the reorientation of the initially {111} surfaces to {100} surfaces of a higher energy with a reorientation of the NW cross section changing from rhombic to square, eventually leading to a ⟨100⟩/{100} NW after ∼40% tensile strain. The geometric reorientation of the cross section from rhombic to square and the ∼40% tensile strain required to

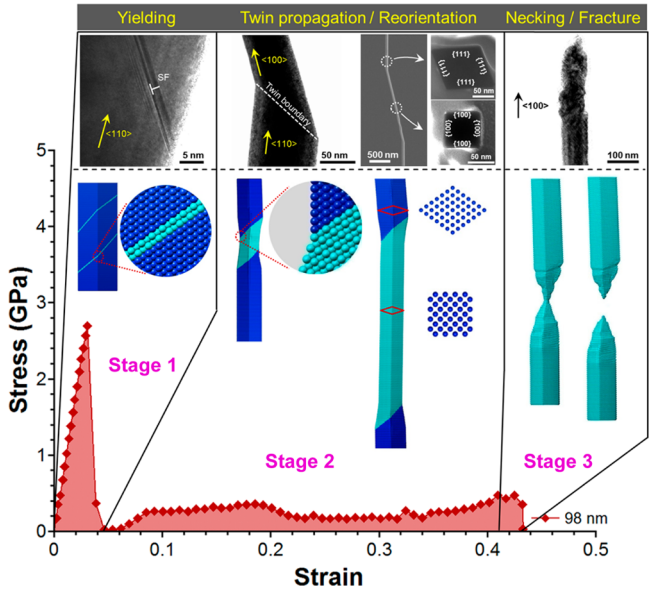

Figure 1. Three distinct stages of uniaxial tensile deformation for a representative Pd NW with a diameter of 98 nm. Stage 1: elastic deformation of an initially ⟨110⟩/{111} rhombic NW. Nanotwins composed of stacking faults were nucleated upon abrupt load drop as shown in the inset. SF represents stacking faults. Stage 2: twin propagation and concurrent reorientation of the rhombic ⟨110⟩/{111} NW to a square ⟨100⟩/{100} NW (see Supporting Information Figure S1 for SAED patterns). The long-range order coherent twin propagation results in about 40% elongation. Stage 3: deformation and eventual fracture of a reoriented ⟨100⟩/{100} NW (see also Supporting Information Movies S1 and S2).

complete the process matches with the 41% strain predicted by MD simulations.[19] This reorientation strain of 41% is also important because it is about 1 order of magnitude longer than observed in conventional bulk shape memory alloys such as NiTi.[20−22] Finally, after the reorientation process is complete linear elastic deformation of the resulting ⟨100⟩/{100} NW proceeds during a fracture stage (stage 3). Yield of the reoriented ⟨100⟩/{100} NW occurs via the nucleation and propagation of full and partial dislocations, as previously observed in MD simulations and experiment,[9,23,24] leading to fracture after about 3.1% strain of the ⟨100⟩/{100} NW, and a total of 43.5% strain for the initial ⟨110⟩/{111} NW. This fracture strain of nearly 50% demonstrates that these rhombic ⟨110⟩/{111} metal NWs are exceptionally ductile.

Figure 2 shows complete stress−strain curves for the ⟨110⟩/{111} Pd NWs with diameters of 40−182 nm. Importantly, while twin propagation induced ductility with about 50% strain is observed regardless of the NW diameter, it is clearly seen that there is size-dependence both in the yield stress of the ⟨110⟩/{111} NWs and in the twin propagation stress which drives the reorientation of the NW from ⟨110⟩/{111} to ⟨100⟩/{100}.

We first discuss the size-dependence of the yield stress for the ⟨110⟩/{111} Pd NWs in Figure 3, where the yield stresses from stage 1 in Figure 2 are plotted with respect to the NW diameters. The yield stress increases as the NW diameters decreases down to 40 nm at which point it reaches a value of 4 GPa, which is an order of magnitude higher than the bulk yield stress. By fitting the yield strength to the standard power-law form $\sigma_y \propto d^{-n}$, we obtain $n \sim 0.61$, where d is the NW diameter and σ_y is the yield stress. This n value falls into the range of 0.5−1, which is typically reported for fcc metals including Al,

dx.doi.org/10.1021/nl402282n | Nano Lett. 2013, 13, 5112−5116

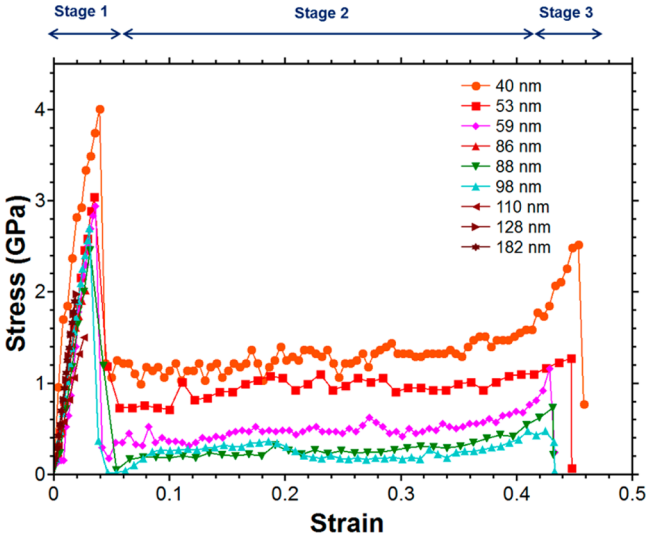

Figure 2. Stress−strain curves for initially ⟨110⟩/{111} Pd NWs with diameters 40−182 nm.

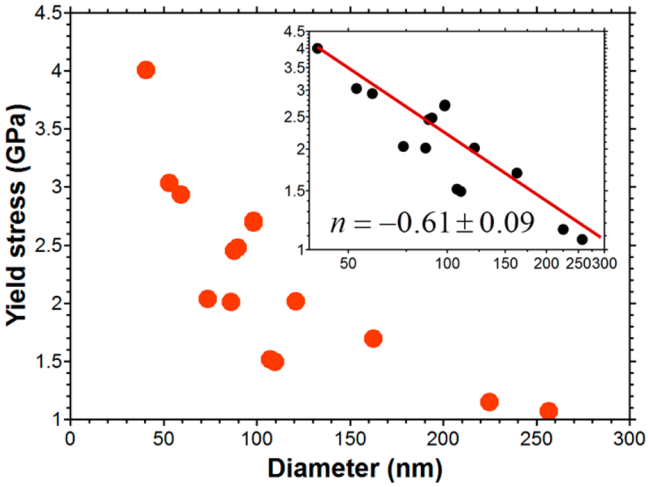

Figure 3. Size-dependence of the yield stress for the ⟨110⟩/{111} Pd NWs captured from the stage 1 in Figure 2

Cu, Ni, Au, and so forth.[3] The variation of the power law exponent, which is also called the size-dependent exponent, has previously been associated with bulk deformation mechanisms such as dislocation nucleation and dislocation forest cutting. In our study, we have clearly shown that the deformation mechanism in tension is the nucleation of partial dislocations at the vertices (surface) of the rhombic cross section, which propagate across the NW cross section on a {111} slip plane.[23−25] Hence, we show that instead of the strengthening mechanism being that of multiplication or interaction of dislocations as for bulk polycrystalline metals, the stress required to nucleate the partial dislocation from the surface (corresponding to the yield stress) increases by decreasing the NW diameter, which gives the size-dependent exponent $n \sim 0.61$. Our power law exponent is indeed similar to the exponent of 0.66 obtained by Zhu et al.,[13] though their Ag NWs were ⟨110⟩ wires with a pentagonal cross section and 5-fold twin symmetry. Similar to them, we believe that an increase in the NW stiffness may be one reason for the reduced power law exponent as we also observed an increase in stiffness with decreasing NW diameter as shown in Figure 2.

More importantly, we report, for the first time in Figure 4, a clear size-dependence of the twin propagation behavior, where

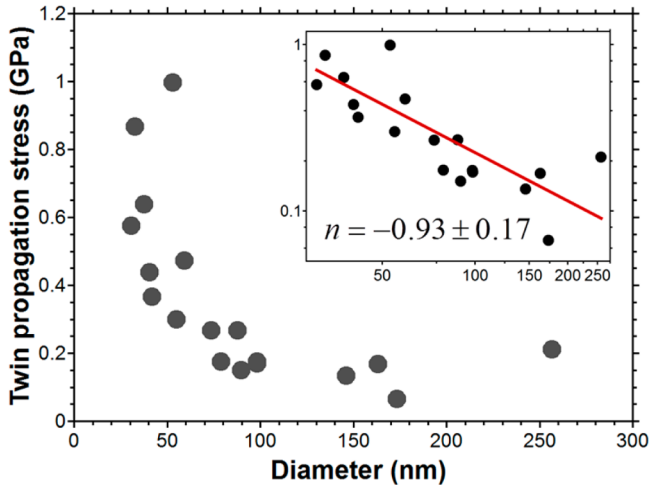

Figure 4. Size-dependence of the twin propagation stress during the ⟨110⟩/{111} to ⟨100⟩/{100} reorientation for Pd NWs captured from the stage 2 in Figure 2

the twin propagation stress was determined by averaging the stress between the strains of 0.1−0.4 in Figure 2. At a critical diameter of about 100 nm, the twin propagation stress begins to increase substantially. Specifically, the twin propagation stress increases nearly 5-fold from about 0.2 GPa to about 1 GPa as the NW diameter decreases from 100 to 30 nm. Furthermore, we find that if the twin propagation stress is analyzed in power-law format, that is, $\sigma_{tm} \propto d^{-n}$, where σ_{tm} is the twin propagation stress, the exponent we find is n close to unity ($n = 0.93$). The $1/d$ dependence for the twin propagation stress was predicted theoretically but until now has not been observed experimentally before. We explain this exponent value following the micromechanical theory presented by Liang et al.[25] and the surface energy differential model of Li et al..[15] As shown in the Supporting Information, the twin propagation stress can be written as $\sigma_{tm} = K/d$, where K is a geometric factor of the surface reorientation. We have derived the lattice reorientation factor K for the rhombic single crystalline ⟨110⟩/{111} fcc NW as in the surface energy differential model as

$$K = \frac{4\sqrt{3}\left(\gamma_{100} - \frac{\sqrt{3}}{2}\gamma_{111}\right)}{(\sqrt{2} - 1)} \quad (1)$$

We show in Figure 5 a comparison between the analytical surface energy differential model in equation 1 with the twin propagation stress measured experimentally in the present work for three different ⟨110⟩/{111} NWs, that is, Au (red stars), Pd (gray solid circles), and AuPd (orange diamonds). We note that the data for the Au and AuPd NWs fall within a narrower size range due to experimental difficulties in synthesizing these NWs with very small and very large diameters. As can be seen, the analytical model with the inverse diameter relationship captures the size-dependent twin propagation stress very accurately, where the slight difference between the model and experiment may be because we ignore the dissipation stress, which is typically less than 100 MPa,[15] possible errors in the surface energy values, or torque caused by grip constraints in the experimental setup, where more detailed discussions are provided in the Supporting Information.

dx.doi.org/10.1021/nl402282n | Nano Lett. 2013, 13, 5112−5116

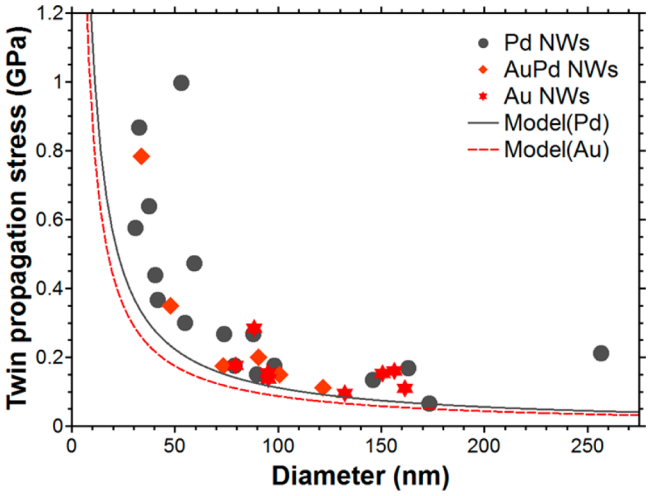

Figure 5. Comparison of the analytical surface energy differential model in eq 1 vs experimental data for the twin propagation stress, as measured during the ⟨110⟩/{111} to ⟨100⟩/{100} reorientation process.

Interestingly, the twin propagation stresses of the AuPd and Au overlap (Figure 5). The similarity of the size-dependence for the three different NWs (Au, Pd, and AuPd) can be explained by the similar difference in surface energies from {111} to {100} that is characteristic of fcc metals.[27,28] The surface energy obtained from GGA calculations for the {111} and {100} surfaces of Pd are 1.92 and 2.33 J/m^2, while the same surfaces of Au have energies 1.28 and 1.63 J/m^2, respectively.[28] While the surface energies of Pd are about 50% higher than those of Au for a given orientation, the K value for Pd (11.16 J/m^2) is closer (~28% difference) to that for Au (8.72 J/m^2), which results in the similar twin propagation stress at a given diameter as illustrated by the gray solid line and red dotted line in Figure 5. This result shows the validity of our model and also demonstrates the increasing importance of surface energy on the twin propagation stress with decreasing NW diameter. This surface energy differential model predicts a twin propagation stress of around 3.4 GPa for NWs having diameters of 2−5 nm, which is similar to that predicted for metal NWs using MD simulations.[16,17,26] Such high twin propagation stress for NWs with small diameters insinuates the high energy storage application of single crystalline metal NWs using its unique deformation twinning behavior and shape memory properties as proposed in previous simulations.[15−18]

In conclusion, this study clarified the size-dependent twin propagation behavior of metal NWs. The key findings can be summarized as follows: First, for defect-free single crystalline Pd NWs, we observed ultrastrong and ductile behavior as a result of coherent twin propagation regardless of the NW diameter. Second, we clearly showed for the first time that the size-dependent behavior of twin propagation is distinctly different from that of initial yielding, where the inverse proportionality of twin migration stress with diameter (size-dependent exponent $n \sim 1$) can be explained by a surface energy differential model. Finally, we showed that the twin propagation stress increases more dramatically with decreasing NW diameters than the yield stress, demonstrating the fundamental role that surface reorientations play in enhancing the size-dependent mechanical behavior and properties of metal NWs.

Our results also imply the possibility of the energy storage application of single crystalline metal NWs using this unique deformation twinning behavior.

■ ASSOCIATED CONTENT

Ⓢ Supporting Information

In situ mechanical testing movies showing twin propagation of Pd NW (Movie S1) and force-measurement during tensile test (Movie S2) are provided. The derivation of surface energy differential model (equation 1) and the experimental results of yield strength of Au, Pd, and AuPd NWs are also available. This material is available free of charge via the Internet at http://pubs.acs.org.

■ AUTHOR INFORMATION

Corresponding Authors

*E-mail: (J.P.A.) jpahn@kist.re.kr.
*E-mail: (B.K.) bongsoo@kaist.ac.kr.
*E-mail: (I.S.C.) insukchoi@kist.re.kr.

Author Contributions

[▽]J.-H.S. and H.S.P. contributed equally to this work.

Notes

The authors declare no competing financial interest.

■ ACKNOWLEDGMENTS

This work was supported by KIST R&D program of 2Z03770 (ISC), NSF grant CMMI-1036460 (HSP), NSF DMR-1240933 (JL), Pioneer Research Center Program through NRF funded by the MEST, Korea (2012-0001059), and the Public Welfare & Safety research program through NRF-2012M3A2A1051686.

■ REFERENCES

(1) Park, H. S.; Cai, W.; Espinosa, H. D.; Huang, H. *MRS Bull.* **2009**, *34*, 178−183.
(2) Greer, J. R.; Hosson, J.; Th, M. D. *Prog. Mater. Sci.* **2011**, *56*, 654−724.
(3) Kraft, O.; Gruber, P. A.; Mönig, R.; Weygand, D. *Annu. Rev. Mater. Res.* **2010**, *40*, 293−317.
(4) Weinberger, C. R.; Cai, W. *J. Mater. Chem.* **2012**, *22*, 3277−3292.
(5) Richter, G.; Hillerich, K.; Gianola, D. S.; Mönig, R.; Kraft, O.; Volkert, C. A. *Nano Lett.* **2009**, *9*, 3048−3052.
(6) Yoo, Y.; Seo, K.; Han, S.; Varadwaj, K. S. K.; Kim, H. Y.; Ryu, J. H.; Lee, H. M.; Ahn, J. P.; Ihee, H.; Kim, B. *Nano Lett.* **2010**, *10*, 432−438.
(7) Yoo, Y.; Yoon, I.; Lee, H.; Ahn, J.; Ahn, J. P.; Kim, B. *ACS Nano* **2010**, *4*, 2919−2927.
(8) Zheng, H.; Cao, A.; Weinberger, C. R.; Huang, J. Y.; Du, K.; Wang, J.; Ma, Y.; Xia, Y.; Mao, S. X. *Nature Commun.* **2010**, *1*, 144.
(9) Seo, J.-H.; Yoo, Y.; Park, N.-Y.; Yoon, S.-W.; Lee, H.; Han, S.; Lee, S.-W.; Seong, T.-Y.; Lee, S.-C.; Lee, K.-B.; Cha, P.-R.; Park, H. S.; Kim, B.; Ahn, J.-P. *Nano Lett.* **2011**, *11*, 3499−3502.
(10) Yue, Y.; Liu, P.; Zhang, Z.; Han, X.; Ma, E. *Nano Lett.* **2011**, *11*, 3151−3155.
(11) Lu, Y.; Song, J.; Huang, J. Y.; Lou, J. *Adv. Funct. Mater.* **2011**, *21*, 3982−3989.
(12) Sedlmayr, A.; Bitzek, E.; Gianola, D. S.; Richter, G.; Mönig, R.; Kraft, O. *Acta Mater.* **2012**, *60*, 3985−3993.
(13) Zhu, Y.; Qin, Q.; Xu, F.; Fan, F.; Ding, T.; Zhang, T.; Wiley, B. J.; Wang, Z. L. *Phys. Rev. B* **2012**, *85*, 045443.
(14) Wu, B.; Heidelberg, A.; Boland, J. J. *Nat. Mater.* **2005**, *4*, 525−529.
(15) Li, S.; Ding, X.; Li, J.; Ren, X.; Sun, J.; Ma, E. *Nano Lett.* **2010**, *10*, 1774−1779.
(16) Park, H. S.; Gall, K.; Zimmerman, J. A. *Phys. Rev. Lett.* **2005**, *95*, 255504.

(17) Liang, W.; Zhou, M. *Nano Lett.* **2005**, *5*, 2039−2043.
(18) Park, H. S.; Gall, K.; Zimmerman, J. A. *J. Mech. Phys. Solids* **2006**, *54*, 1862−1881.
(19) Liang, W.; Zhou, M. *Phys. Rev. B* **2006**, *73*, 115409.
(20) Gall, K.; Sehitoglu, H.; Chumlyakov, Y. I.; Kireeva, I. V. *Acta Mater.* **1999**, *47*, 1203−1217.
(21) Liu, Y.; Xie, Z.; Van Humbeeck, J.; Delaey, L. *Acta Mater.* **1998**, *46*, 4325−4338.
(22) Gall, K.; Maier, H. J. *Acta Mater.* **2002**, *50*, 4643−4657.
(23) Diao, J.; Gall, K.; Dunn, M. L. *Nano Lett.* **2004**, *4*, 1863−1867.
(24) Park, H. S.; Zimmerman, J. A. *Phys. Rev. B* **2005**, *72*, 054106.
(25) Leach, A. M.; McDowell, M.; Gall, K. *Adv. Funct. Mater.* **2007**, *17*, 43−53.
(26) Liang, W.; Srolovitz, D. J.; Zhou, M. *J. Mech. Phys. Solids* **2007**, *55*, 1729−1761.
(27) Wan, J.; Fan, Y. L.; Gong, D. W.; Shen, S. G.; Fan, X. Q. *Model. Simul. Mater. Sci. Eng.* **1999**, *7*, 189−206.
(28) Vitos, L.; Ruban, A. V.; Skriver, H. L.; Kollár, J. *Surf. Sci.* **1998**, *411*, 186−202.